

PAPER • OPEN ACCESS

An updated set of electron-impact cross sections for CO₂: untangling dissociation and application to CO₂ with Ar and N₂ admixtures

To cite this article: Yang Liu *et al* 2025 *Plasma Sources Sci. Technol.* **34** 035003

View the [article online](#) for updates and enhancements.

You may also like

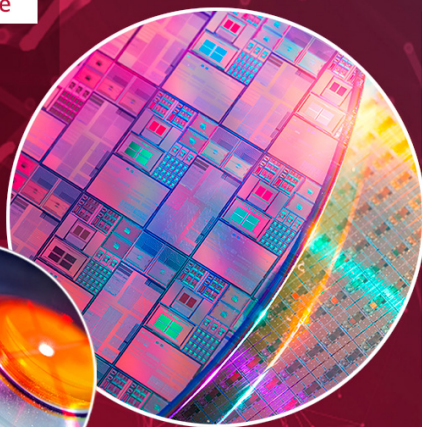
- [Collision integrals of electronically excited atoms in air plasmas: II. N–O interactions](#)
Wensheng Zhao, Qizhen Hong, Chao Yang *et al.*
- [A deep learning approach for electric field profile reconstruction based on the E-FISH method](#)
Zhijian Yang, Edwin Setiadi Sugeng and Tat Loon Chng
- [Computational study of characteristics of atmospheric pressure glow discharge in helium](#)
Gubad Islamov, Ender Eylenceoglu and Ismail Rafatov

Analysis Solutions for your **Plasma Research**

HIDEN
ANALYTICAL

For Surface Science

- ▶ Surface Analysis
- ▶ SIMS
- ▶ 3D depth Profiling
- ▶ Nanometre depth resolution



For Plasma Diagnostics

- ▶ Plasma characterisation
- ▶ Customised systems to suit plasma Configuration
- ▶ Mass and energy analysis of plasma ions
- ▶ Characterisation of neutrals and radicals



[Click to view our product catalogue](#)

■ Knowledge
■ Experience ■ Expertise

Contact Hiden Analytical for further details:

 www.HidenAnalytical.com
 info@hiden.co.uk

An updated set of electron-impact cross sections for CO₂: untangling dissociation and application to CO₂ with Ar and N₂ admixtures

Yang Liu^{1,2} , Tiago Silva² , Tiago C Dias^{2,3} , Pedro Viegas² , Xiangen Zhao⁴ , Yaping Du⁴, Junjia He¹ and Vasco Guerra^{2,*} 

¹ State Key Laboratory of Advanced Electromagnetic Technology, School of Electrical and Electronic Engineering, Huazhong University of Science and Technology, Wuhan 430074, People's Republic of China

² Instituto de Plasmas e Fusão Nuclear, Instituto Superior Técnico, Universidade de Lisboa, Lisboa 1049-001, Portugal

³ Department of Electrical Engineering and Computer Science, University of Michigan, Ann Arbor, MI 48109-2122, United States of America

⁴ Department of Building Environment and Energy Engineering, The Hong Kong Polytechnic University, Hong Kong Special Administrative Region of China 999077, People's Republic of China

E-mail: vguerra@tecnico.ulisboa.pt

Received 30 October 2024, revised 5 February 2025

Accepted for publication 26 February 2025

Published 10 March 2025



CrossMark

Abstract

This work proposes an updated set of electron-impact cross sections (CSs) for carbon dioxide (CO₂) by quantitatively identifying CO₂ dissociation within the two electronic excitation channels proposed by Phelps. In particular, the CS with energy threshold at 7 eV is considered with a 15% dissociation branching ratio and is associated with dissociation into O(¹D) + CO(X), while the one with threshold at 10.5 eV is used entirely for dissociation into O(³P) + CO(a³Π_r). Experimental data on CO₂ dissociation rate coefficients at moderate reduced electric field (E/N), CO₂ conversion efficiencies at high E/N , and electron transport coefficients for $E/N \in [10^{-2}, 10^3]$ Td are used to validate the updated set and demonstrate its completeness and consistency over a wide range of E/N . Notably, the updated CS set enables the full coupling between the electron and chemical kinetics, a feature lacking in most existing CS sets. The updated set is applied to study electron kinetics in CO₂-Ar and CO₂-N₂ mixtures, revealing significant modifications in the electron energy distribution function and CO₂ dissociation rate coefficient due to mixture composition. The updated CS set is made available at the IST-Lisbon database within LXCat.

Keywords: carbon dioxide, electron-impact cross section, CO₂ dissociation, Ar and N₂ admixtures, electron kinetics

* Author to whom any correspondence should be addressed.



Original content from this work may be used under the terms of the [Creative Commons Attribution 4.0 licence](https://creativecommons.org/licenses/by/4.0/). Any further distribution of this work must maintain attribution to the author(s) and the title of the work, journal citation and DOI.

1. Introduction

In recent years, non-thermal plasma technology has been widely applied to CO₂ conversion to achieve the goal of net-zero carbon emissions on Earth [1–4] and *in-situ* resource utilization (ISRU) on Mars [5–8]. This interest is due to the abundant reactive radicals in non-thermal plasma (e.g. electron, excited state particles, and oxygen atoms) and the ability to couple renewable energy for power supply, providing a promising way to convert the thermally stabilized CO₂ molecule with high energy and cost efficiencies [4, 9–11]. In addition, the synergistic effect of plasma and catalyst increases the confidence in the industrial application of plasma-assisted CO₂ conversion [12–17].

Electron-impact collisions are at the origin of all plasma chemistry processes, as they transfer the electron energy obtained from the electric field into heavy particles that start the subsequent chemistry reactions [9, 18–20]. The corresponding electron-impact cross sections (CSs) are the most fundamental parameter determining electron kinetics, quantifying the probability that the electron has a specific type of collisions [21, 22]. In particular, the profile and energy threshold of the CS define the selectivity to various collisional channels. Therefore, a reliable set of electron-impact CSs, serving as critical input to the electron Boltzmann equation [23–27] or a Monte-Carlo code [28–30], is essential to accurately characterize the electron energy distribution function (EEDF) and the electron transport coefficients.

A complete and consistent set of electron-impact CSs for CO₂, including effective momentum transfer, dissociative attachment, vibrational excitation, electronic excitation and ionization processes, was proposed and published in the IST-Lisbon database with LXCat a few years ago [31–33]. This set was validated by comparison with measured values of electron transport coefficients and was widely used to investigate the electron and heavy-particle kinetics in different discharge conditions both in pure CO₂ and in mixtures of CO₂ with other gases [34–40]. However, an important uncertainty was pointed out, namely that the electron-impact dissociation CS is not unambiguously identified [31]. The other complete and consistent CS sets available in LXCat share the same uncertainty, except for the Biagi database [41], which distinguishes several dissociation and excitation channels.

Since the 1960s, several sets for electron-impact CO₂ dissociation CSs have been proposed, *e.g.* by Polak and Slovetsky [42], Itikawa [43], Cosby and Helm [44], and Corvin and Corrigan [45], supported by experiments or theoretical calculations. Phelps and co-workers [46] proposed two electronic excitation CSs by analysing electron transport coefficients, with energy thresholds at 7 and 10.5 eV and denoted here as Phelps_7_eV and Phelps_10.5_eV, respectively. Each of these CSs has already been used in the literature as representative of dissociation to assess the CO₂ dissociation performance by electron-impact reactions [31, 47–50]. The choice of dissociation CS to reproduce the measured CO₂ conversion has been a long-standing challenge [51, 52], that remains open. Indeed,

the dissociation rate coefficients calculated from different dissociation CSs can span over a few orders of magnitude [31].

Measurements of dissociation rate coefficients make it possible to assess and validate the accuracy of electron-impact CO₂ dissociation CSs. Corvin and Corrigan [45] showed CO₂ dissociation rate coefficients as a function of reduced electric field (E/N) by separating and measuring the non-condensable products formed in positive column glow discharges. With a ‘building-up’ experiment in static conditions, Morillo-Candas *et al* [53] reported the latest measured results of CO₂ dissociation rate coefficients in the range of 40 Td to 110 Td.

From the comparison of Boltzmann calculations and the experimental data from [53], Grofulović *et al* [31] noted that the CSs for electronic excitation in the IST-Lisbon database, based on the work by Phelps and co-authors [46], most likely include not only dissociative channels but also some additional contributions. To circumvent this difficulty, it was suggested that the CO₂ dissociation rate coefficient should be calculated using Polak and Slovetski’s dissociation CSs [42], which is neither used to obtain the EEDF nor it is part of the IST-Lisbon dataset, upon integration of a previously calculated EEDF [31]. This procedure brought a considerable success in the self-consistent modelling of CO₂ plasmas [34, 37, 54–56], but remains somewhat unsatisfactory as the CSs used to obtain the EEDF are not the same used in the rate-balance equations for the heavy-species.

By comparing the calculated CO₂ conversions using different dissociation CSs with the measured values in dielectric barrier discharge (DBD) and microwave (MW) plasmas, Bogaerts *et al* [48] suggested that the CS proposed by Polak [42] and Itikawa [43] would underestimate CO₂ conversion, and reinforced that the CS proposed by Phelps [46] would include more than just dissociation and possibly electronic excitation channels as well. Pietanza *et al* [49, 50] recommended the utilization of the excitation CS Phelps_7_eV for dissociation, and the excitation CS Phelps_10.5_eV for electronic excitation. Vialetto *et al* [57] assumed the CS by Biagi [41] with a 50% dissociation factor and showed a good agreement between the calculated and measured [53] CO₂ dissociation rate coefficients at moderate E/N between 60 and 110 Td. Babaeva and Naidis [47] demonstrated the accuracy of the Phelps_10.5_eV CS as the main dissociation channel at $E/N > 90$ Td, by comparing and analysing CO₂ conversion efficiencies with different dissociation CSs in DBD and streamer discharges. In addition, the essential role of electronically excited states for gas heating was addressed in [58], and a feedback mechanism for the energy of CO₂ electronic excitation channel in fast gas heating was suggested by Biondo *et al* [59] in CO₂ pulse discharges. All these studies indicate that both electronic excitation and dissociation channels need to be included in a complete and consistent set of electron-impact CSs for CO₂, and the accuracy of the CO₂ dissociation CSs should be verified over a wide range of E/N .

The motivation to study the effects of Ar and N₂ additions on CO₂ plasmas stems first and foremost from the new field of plasma ISRU, as the gas composition in the Martian

atmosphere is approximately 95%CO₂–3%N₂–2%Ar [60, 61]. In addition, Ar is usually added to CO₂ plasmas for spectral diagnostics of electron density and temperature [62, 63], and N₂ is a major component in industrial flue gases on earth [64, 65]. Finally, it has been proved that the additions of N₂ and Ar play a beneficial role in the plasma-assisted CO₂ conversion [66–71]. For instance, optical emission spectroscopy studies revealed an increase in the electron density with the Ar fraction in CO₂–Ar mixtures [72, 73], while an increase of absolute CO₂ conversion was found in CO₂–N₂ mixtures [37, 66], that has been justified by vibrational energy exchanges in CO₂–N₂ and CO–N₂ collisions [37, 74], gas dilution and limitation in the inverse reactions [71, 75], and modifications in the EEDF [55, 76]. Despite significant insight on the elementary phenomena underlying the kinetics in CO₂ with Ar and N₂ admixtures already achieved [37, 77], the lack of systematic investigations into electron kinetics in these mixtures, particularly the uncertainties surrounding the CO₂ dissociation CS, has hindered further development of chemical kinetics schemes and plasma fluid models.

In this work, we capitalize on the results from [31] to propose an updated set of electron-impact CSs that quantitatively identifies the CO₂ dissociation in the electronic excitation channels. This set gives results in excellent agreement with measured values of CO₂ dissociation rate coefficients, CO₂ conversion efficiencies and electron transport coefficients, over a wide range of E/N , and will be made available at the IST-Lisbon database within LXCat. Furthermore, we use the updated CS set to investigate the effects of mixture compositions and vibrational excitation degree on the electron kinetics in CO₂ plasmas with Ar and N₂ admixtures.

The structure of this paper is as follows: section 2 presents the detailed set of electron-impact CO₂ dissociation CSs and the validation with measured values for a wide range of E/N . Section 3 evaluates and recommends an updated complete and consistent set of electron-impact CSs for CO₂ to study electron kinetics and plasma chemistry. In section 4, the application of the updated CS set is extended to address the electron kinetics in CO₂ plasmas with Ar and N₂ admixtures. Finally, the concluding remarks are summarized in section 5.

2. Electron-impact CO₂ dissociation CSs

2.1. Overview

Direct electron-impact dissociation is regarded as one of the most critical pathways for CO₂ conversion in non-thermal plasmas [9] and its dissociation rate coefficient directly depends on the electron-impact CO₂ dissociation CS considered. Figure 1 illustrates several CSs suggested or used by different researchers as representative of CO₂ dissociation (see also discussion in [31]). Phelps and co-workers [46] proposed two electronic excitation CSs that are often associated with dissociation [31, 47–50]. Polak and Slovetsky [42] developed a method to compute two dissociation CSs for

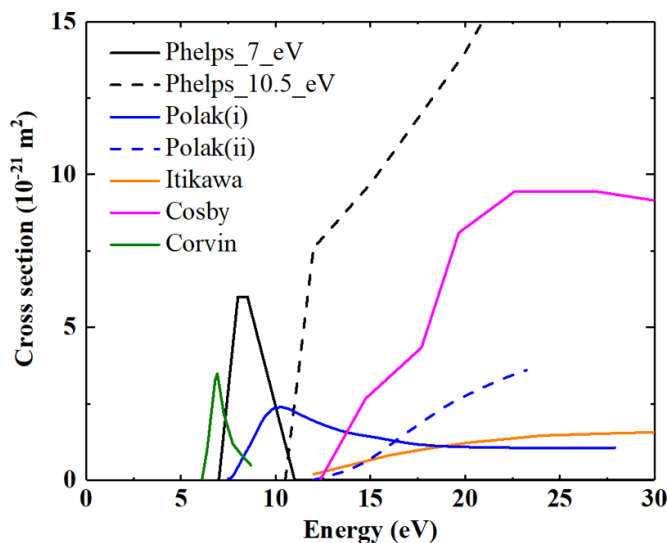


Figure 1. Electron-impact CO₂ dissociation cross sections proposed by different researchers [42–46].

CO₂: Polak(i), which corresponds to a dissociation channel by excitation of allowed transitions from a set of electronically excited states with threshold ~ 7 –9 eV, and Polak(ii), associated with the formation of CO($a^3\Pi_r$). The CSs proposed by Cosby [44] and Itikawa [43] were based on absolute measurements of partial dissociation channels and adopted a total CS to represent all dissociation channels. These two CSs have higher energy thresholds compared with those from Phelps and Polak, as shown in figure 1. The CS estimated by Corvin [45] is a construction derived by inverting the measured CO₂ dissociation rate coefficients, assuming a Maxwellian EEDF.

A comparison between the calculated CO₂ dissociation rate coefficients using different dissociation CSs with the latest experimental data [53] indicates that the rate coefficients obtained from the Cosby [44] and Itikawa [43] CSs are two orders of magnitude lower than the measured values. Although the rate coefficients obtained from Corvin CS [45] align with measurements at low E/N , they underestimate the rate coefficients at $E/N > 90$ Td, and lack physical meaning, being only a mathematical construction as a solution to a (significantly) under-constrained inverse problem. Therefore, the CSs proposed by Cosby, Itikawa, and Corvin are not considered in this work.

The CO₂ conversion and relative product fractions predicted using Polak CSs in a self-consistent kinetic model for low-pressure DC glow discharges align with measured values [34, 37, 54–56]. Although Polak CSs have proved to describe accurately electron-impact dissociation in these conditions, they are not part of complete and consistent CS sets and, hence, are not used to date for analysing electron transport coefficients [31, 48]. Moreover, it has been shown that they underestimate dissociation at high E/N [47]. Phelps CSs tend to overestimate CO₂ conversion, because they account for all

Table 1. Test cases of CO₂ dissociation CSs used for comparing dissociation rate coefficients.

Case	CS for electron-impact CO ₂ dissociation reactions	
	$e + \text{CO}_2(\text{X}) \rightarrow e + \text{CO}(\text{X}) + \text{O}({}^1\text{D})$	$e + \text{CO}_2(\text{X}) \rightarrow e + \text{CO}(\text{a}^3\Pi_r) + \text{O}({}^3\text{P})$
A: Polak CSs [42]	Polak(i)	Polak(ii)
B: Phelps CSs [46]	Phelps_7_eV	Phelps_10.5_eV
C: Phelps 50% diss. factor	50%* Phelps_7_eV	Phelps_10.5_eV
D: Phelps 15% diss. factor	15%* Phelps_7_eV	Phelps_10.5_eV
E: hybrid	Polak(i)	Phelps_10.5_eV

the electronic excitation channels and not only dissociation [48]. However, their excellent performance at high E/N [47] and their use in the analysis of electron transport coefficient as part of a validated CS set [31] motivates further study and refinement of this CS set.

We suggest to consider the Phelps CSs as describing not only dissociation but also electronic excitation, and to introduce a dissociation factor to quantitatively identify the corresponding branching ratio in the excitation channels. In principle, such procedure must lead to exactly the same EEDFs and electron transport coefficients as obtained with the initial CS set from [31], as it is shown and discussed in section 3. In addition, given the widespread adoption and reliable predictions obtained with Polak's dissociation CSs in previous studies [34, 37, 54–56], in section 2.2 we compare and analyse the differences in CO₂ dissociation rate coefficients and CO₂ conversion efficiency when using Polak CSs and the present approach.

2.2. Assessment and validation

Table 1 shows the test cases of CO₂ dissociation CSs used here for comparing the corresponding CO₂ dissociation rate coefficients. The Phelps_10.5_eV CS is assumed to describe dissociation forming O(³P) and CO(a³Π_r) [39, 56]. It is the dominant CO₂ dissociation channel and provides a good calculation of the CO₂ conversion efficiency at high E/N [47]. In turn, the incorporation of Phelps_7_eV CS overestimates dissociation at E/N below ~110 Td [31]. Therefore, we consider a dissociation factor, defined as the fraction of the Phelps_7_eV CS that leads to dissociation producing CO(X) and O(¹D), with the rest allocated to electronic excitation, that correspond to a lumped excitation of several excited states [31, 46]. We have calculated CO₂ dissociation rate coefficients with dissociation factors ranging from 0 to 1 and include here the cases 15% and 50% to highlight the results. Additionally, a 'hybrid case' where the first dissociation channel is described by Polak(i) CS and the second by Phelps_10.5_eV is also taken into account. All calculations in this paper are carried out with the Boltzmann solver LoKI-B of the LisbOn KInetics (LoKI) simulation tool [26].

The CO₂ dissociation rate coefficient, calculated by integrating the CSs considered in the various cases with the EEDFs obtained with the IST-Lisbon CS set [31] at different E/N and for a gas temperature of 300 K, are compared with the experimental data from [45, 53] in figure 2(a). At E/N below 60 Td,

the calculated rate coefficients are lower than the measurements by Corvin and Corrigan [45] for all cases, but there are significant uncertainties associated with pressure changes and the determination of gaseous dissociation products in the experiment [54]. Moreover, the results from Morillo-Candas *et al* [53] under these conditions were performed at higher current and pressure, and thus higher gas temperatures T_g (600–700 K) are reached at the end of the pulses. If we use higher values of the gas and vibrational temperatures in our calculations, the agreement with the experimental data from [53] for $E/N < 60$ Td is noticeably improved, as shown by the dotted line in figure 2(a). At $E/N > 100$ Td, the rate coefficient of the single Phelps_10.5_eV, which is representative of dissociation in this E/N range [47], is always lower than the total dissociation obtained using Phelps (case B), exceeds those from the Polak CSs (case A) and gradually approaches the Phelps CSs with a 15% dissociation factor (case D) (cf as well figure 4 and its discussion).

To facilitate the comparison with the latest measured values at moderate E/N [53], a partial zoom-in in the E/N range from 60 Td to 110 Td is shown in figure 2(b). The measurements fall between the calculated values for the Polak (case A) and Phelps (case B) CSs, confirming that the total Polak CSs lead to an underestimation of CO₂ dissociation at high E/N , while the total Phelps CSs include more than just dissociation [48]. The Phelps CSs with 15% dissociation factor (red curve marked in figure 2) is close to the Polak CSs for E/N below ~80 Td. This observation is of importance, since the Polak CSs were used successfully in the self-consistent modelling of DC discharges with E/N in this range [34, 37, 54–56]. In contrast, both the Phelps CSs with a 50% dissociation factor (case C) and the hybrid CSs (case E) overestimate the CO₂ dissociation rate coefficients. Therefore, by setting a 15% dissociation factor for the Phelps_7_eV CS and adding Phelps_10.5_eV CS to dissociation, the calculated CO₂ dissociation rate coefficients show an excellent agreement with the measured values at moderate E/N .

Figure 3 illustrates the relative contribution of the two dissociation channels to the total CO₂ dissociation rate coefficient versus E/N in case D (Phelps CSs with a 15% dissociation factor). The contribution of the 15% Phelps_7_eV to the CO₂ dissociation rate coefficient by electron impact is above 60% for E/N below 50 Td. For E/N in the 50–110 Td interval, this contribution is reduced to 20%–60% and decreases with the increase in E/N , revealing that the two dissociation channels play a joint role on the rate coefficients in the zoomed-in E/N range of figure 2(b). Once E/N exceeds 200 Td, the

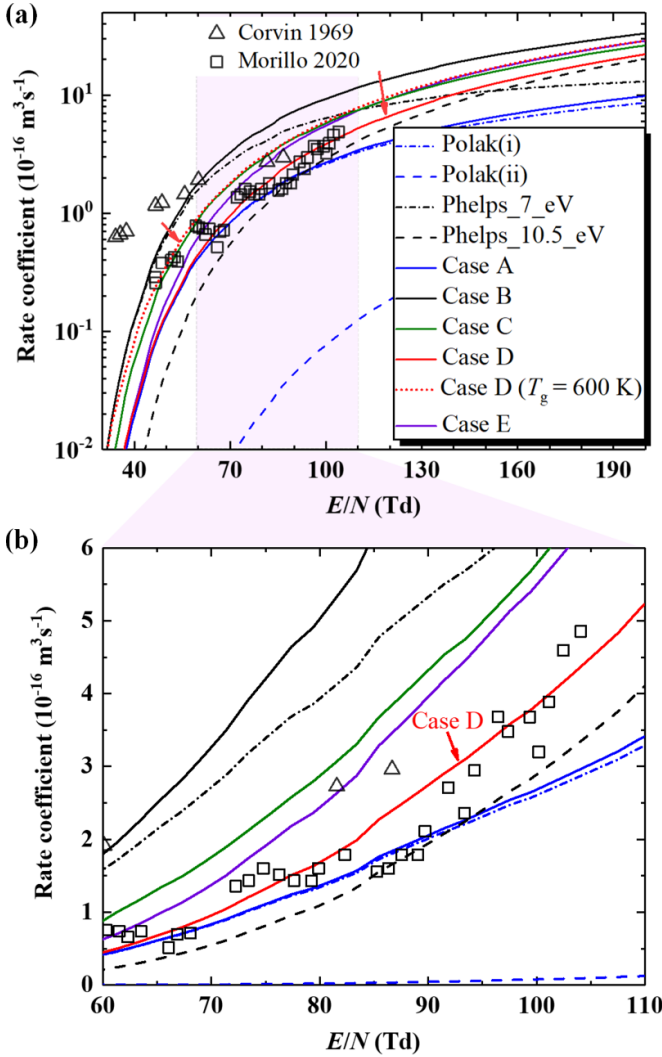


Figure 2. CO₂ dissociation rate coefficients as a function of E/N for various sets of dissociation CSs compared to experiments [45, 53]: (a) E/N in the range of 30–200 Td, (b) enlargement in the range of 60–110 Td.

Phelps_10.5_eV CS becomes the dominant channel for CO₂ dissociation and contributes more than 90% to the dissociation rate coefficient, confirming the importance of this dissociation channel at high E/N pointed out in [47].

The efficiency of CO₂ conversion (G -value), representing the numbers of produced CO species per 100 eV of input energy, is one of the important parameters for evaluating the electron-impact dissociation CS, especially at high E/N [47]. Through the comparison of the calculated G -values using various CO₂ dissociation CSs at 400–600 Td in corona discharges [78, 79], Babaeva and Naidis [47] found that the Phelps_10.5_eV CS leads to the best agreement with the measured values. However, a measured value [80] at 120 Td in DBD is between the results of Phelps_7_eV and Phelps_10.5_eV CSs. Our case D (15% dissociation factor) makes it possible for the calculated G -value to be in good agreement with the measured value in DBD [80], as shown in figure 4. Furthermore, as the contribution of the 15% Phelps_7_eV

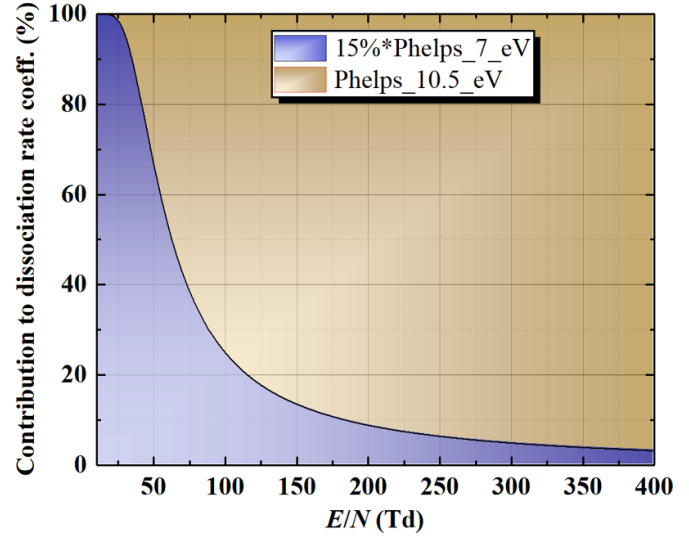


Figure 3. Contributions of two CO₂ dissociation channels to the total CO₂ dissociation rate coefficient in the set of Phelps CSs with a 15% dissociation factor.

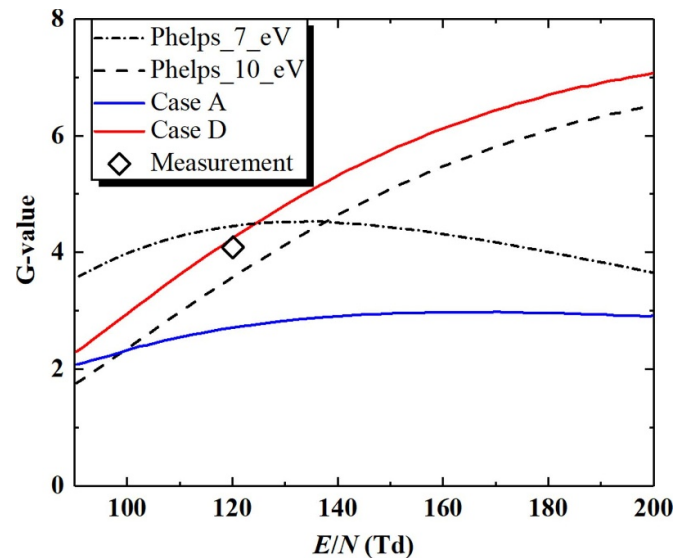


Figure 4. The numbers of produced species per 100 eV of input electric energy (G -values) for CO₂ dissociation by electron impact compared to experiment [80].

channel to CO₂ dissociation in corona discharges of 400–600 Td is below 5% (cf figure 3), the contribution to CO₂ dissociation under these conditions is essentially due to the Phelps_10.5_eV channel. Therefore, combining the data on the CO₂ dissociation rate coefficients at moderate E/N with the CO₂ conversion efficiencies at high E/N , it is confirmed that the Phelps CSs with a 15% dissociation factor (case D) yields results in excellent agreement with the measured values over a wide range of E/N , at least from ~ 50 Td to 400 Td.

It is worth noting that dissociation mechanisms other than direct electron impact have been proposed and studied in the literature. In particular, vibrational-induced dissociation [9, 81] and thermal dissociation [82] have been invoked to

explain observed dissociation degrees in MW and RF discharges. Recent work by Montesano *et al* evinced a delayed dissociation mechanism in nanosecond discharges [83], that is likely a signature of any of these additional dissociation mechanisms. Hence, the question arises whether vibrational-induced and/or thermal dissociation can alter the conclusions of this work. In fact, this is not the case, as it is carefully discussed in [53–55]. The experimental data on the CO₂ dissociation rate coefficient at moderate E/N [53] and the CO₂ conversion efficiency at high E/N [47, 78–80] were all measured at relatively low vibrational excitation degree and gas temperature, and the experiments in [53] were designed to specifically rule out any of these effects.

One additional aspect to consider is the possible role of stepwise electron dissociation. Calculations of stepwise resonant vibrational excitation in CO₂ by Laporta *et al* [84] show an increase of some excitation rate coefficients in transitions $v \rightarrow v + 2$ with the vibrational quantum number v of the bending and asymmetric stretching mode. A possible similar increase in the rate coefficients of stepwise electron impact dissociation may have some impact in the total dissociation rate coefficient, even considering the decrease in the population of the target vibrationally excited states. However, at present there are no reliable data on stepwise dissociation CSs and the estimated differences by including this process fall within the differences between our calculations and the experimental data. This question is discussed and analysed in [55].

3. An updated set of electron-impact CSs

In this section, we update the set of electron-impact CSs based for CO₂ from [31], formerly available at the IST-Lisbon database within LXCat [33], by identifying CO₂ dissociation within the electronic excitation channels. With this paper the new CS set is made available in the same database. Although the utilisation of the previous set in a Boltzmann solver is known to lead to a very good reproduction of the reported measurements of the electron transport coefficients [31], the CO₂ dissociation CSs are not included in the set. This absence means that in the set from [31] the electron kinetics and the EEDFs do not depend explicitly on the CO₂ dissociation CSs.

To couple the electron and the heavy-particle kinetics with the CSs from [31], the rate coefficient of electron-impact CO₂ dissociation (k_{dissoc}) must be obtained by an extra integration of the CSs with a previously calculated EEDF, as illustrated in figure 5(a). In other words, the CSs that are used to study the electron kinetics and obtain the EEDF are *not* the same as the ones used to obtain the electron-impact rate coefficients required to study the chemical kinetics. By employing the setup of Phelps CSs for electronic excitation with a 15% dissociation factor in the Phelps_7_eV CS (see section 2), an updated IST-Lisbon CS set for CO₂ is proposed, that takes into account both electronic excitation and CO₂ dissociation in a straightforward manner. With this updated set of electron-impact CSs for CO₂, all

electronic processes including attachment, elastic collisions, vibrational and electronic excitation, ionization and dissociation can be simultaneously incorporated into the electron Boltzmann equation. Consequently, the EEDF, electron transport coefficients, and all the corresponding rate coefficients of electron-impact reactions can be accurately obtained using this complete set of electron-impact CSs, as depicted in figure 5(b). The new workflow using the updated set enables a full and consistent coupling between the electron and chemical kinetics. It is worth underlining that, by construction, the new set must yield exactly the same EEDF, transport coefficients and electron-impact rate coefficients as the validated set from Grofulović *et al* [31]. This verification is carried out below.

To highlight the consistency of the updated set of electron-impact CSs, the three sets of CSs presented in table 2 are used to analyse the impact of the new approach on the EEDF and electron transport coefficients. Case 1 corresponds to the CS set from [31], in which the total Phelps CSs are regarded as electronic excitation channels rather than dissociation; case 2 incorporates Polak's CSs for dissociation [42] into the previous IST-Lisbon database [31]; in case 3, the updated set divides Phelps_7_eV CS into two distinct CSs, for dissociation producing O(¹D) and electronic excitation, with branching ratios of 15% and 85%, respectively, and utilises the Phelps_10.5_eV CS as an additional dissociation channel to produce CO(*a*³Π_r) (see case D in table 1).

Figures 6(a) and (b) display the calculated EEDFs at 50 Td and 100 Td, respectively. As anticipated, the EEDFs for case 3 are identical to those of case 1: the division of CSs and the modification of collision types do not influence the solution of the electron Boltzmann equation, as the total electron energy transferred in collisions in is the same in both cases. In contrast, the EEDFs for case 2 are lower than those of the other two cases at electron energies exceeding the energy threshold of the 7.5 eV of Polak CSs. This deviation is due to the additional electron energy losses transferred to the dissociation channel described by Polak CSs in case 2, that is not present in the other cases.

The reduced electron mobility and the effective ionization coefficient are calculated and compared with the experimental data from [85–101] in figures 7(a) and (b), respectively. The reduced electron mobility of case 2 is similar to those of cases 1 and 3 (the latter two being again exactly the same), and all three cases give results in good agreement with the measurements [85–96] over the entire range of E/N . The mobility depends mostly on the electrons with low energies and in the body of the distribution, and EEDFs are very similar in these energy ranges (cf figure 6). The slight discrepancy in the calculated values of reduced electron mobility for cases 1 and 2 at $E/N > 100$ Td reflects small changes in EEDFs at the lower electron energies. Regarding the reduced effective ionization coefficient, defined as the subtraction of the attachment coefficient from the Townsend ionization coefficient, the results of cases 1 and 3 are once more confirmed to be the same and match very well the measurements, and case 2 slightly

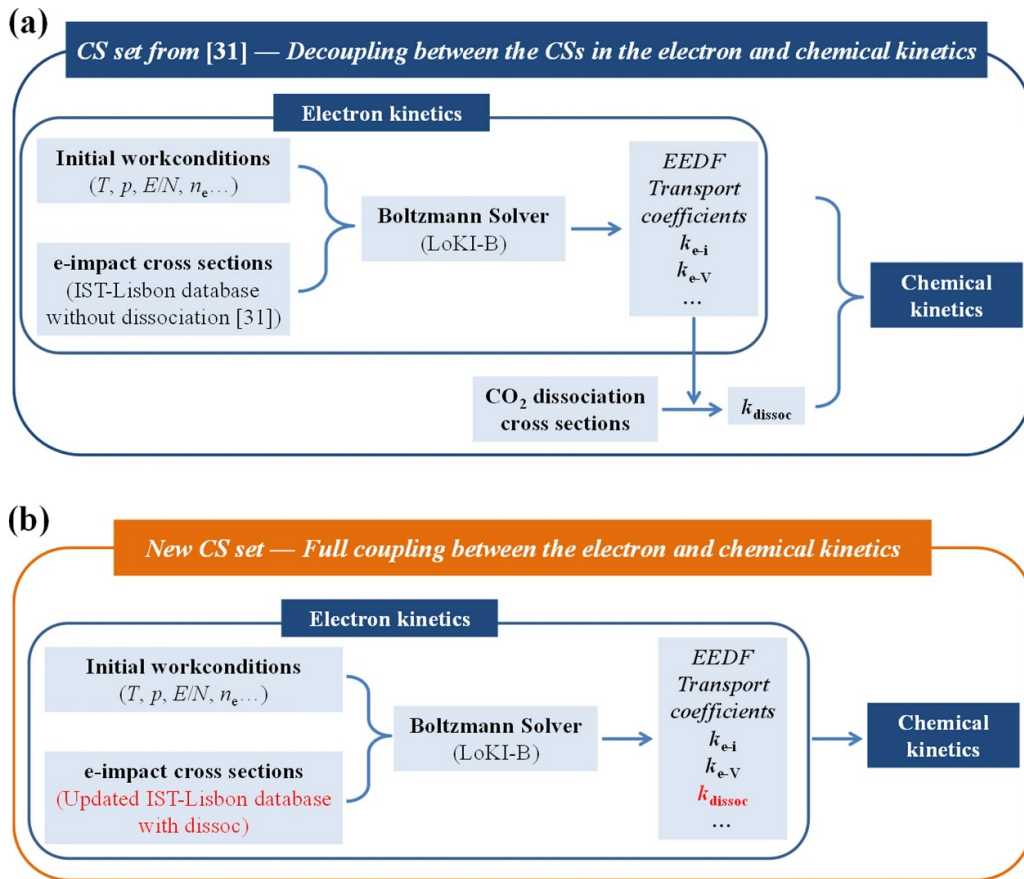


Figure 5. Comparison of solution workflows for coupling the electron and chemical kinetics by adopting (a) the CS set from [31] and (b) the updated CS set from this work.

Table 2. Sets of electron-impact CSs with various CO₂ dissociation CSs based on the complete and consistent set from [31].

Case	Set of electron-impact CSs	Note
Case 1	Former IST-Lisbon database for CO ₂ [31]	Without CO ₂ dissociation CSs
Case 2	Former IST-Lisbon database for CO ₂ [31] + Polak diss. CSs	With CO ₂ dissociation CSs proposed by Polak [42]
Case 3	Present work: updated IST-Lisbon database for CO ₂	Identifying the dissociation in the electronic excitation channels by Phelps [46]

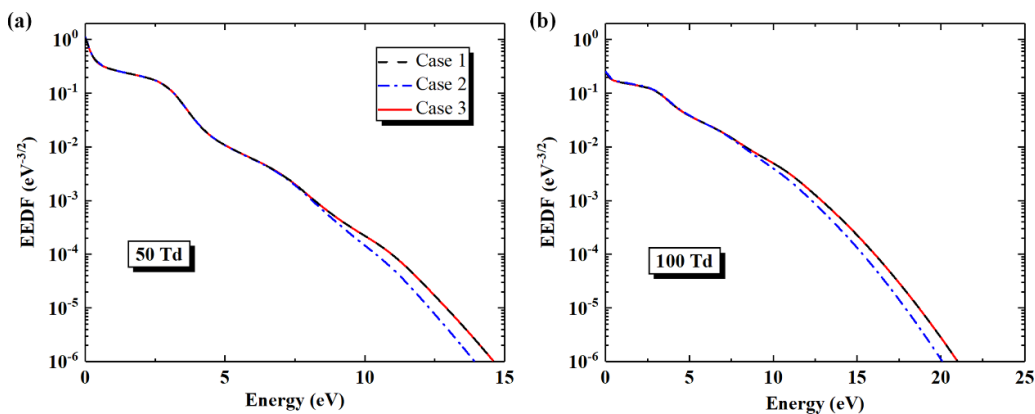


Figure 6. The calculated electron energy distribution functions with the three sets of electron-impact CSs for (a) 50 Td and (b) 100 Td.

underestimates the effective ionization coefficient due to the depletion of the high-energy tail of EEDF.

4. Electron kinetics in CO₂ plasmas with Ar and N₂ admixtures

To extend the application of the updated set of electron-impact CSs for CO₂ presented here, this section investigates the effects of mixture compositions and vibrational excitation degrees on the electron kinetics in CO₂ plasmas with Ar and N₂ admixtures. Furthermore, the impact of the choice of the CO₂ dissociation CSs is emphasized by computing and comparing the corresponding electron-impact rate coefficient, k_{dissoc} , when using different electron-impact CO₂ dissociation CSs in these mixtures. The sets of electron-impact CSs for N₂ and Ar are taken from the IST-Lisbon database [32] on LXCat [33]. The sets for Ar and N₂ were validated by comparing calculated swarm data and rate coefficients with measured values in [102] and [103, 104], respectively.

In this section, $T_{1,2}$ stands for the common vibrational temperature of the CO₂ symmetric stretching and bending modes, T_3 is the vibrational temperature of the CO₂ asymmetric stretching mode and T_{N_2} denotes the vibrational temperature of N₂. We consider two sets of vibrational temperatures: the first one is $T_{1,2} = 500$ K, $T_3 = 1000$ K and $T_{\text{N}_2} = 2000$ K (for CO₂-N₂ mixtures), the second one is $T_{1,2} = 1000$ K, $T_3 = 3000$ K and $T_{\text{N}_2} = 5000$ K (for CO₂-N₂ mixtures). The two cases correspond to typical degrees of vibrational excitation observed under different discharge conditions [37, 70, 71, 105–110]. The population of vibrational levels at different vibrational excitation degrees is assumed to follow a Boltzmann distribution at the corresponding vibrational temperatures.

4.1. CO₂-Ar mixtures

Figures 8(a) and (b) show the EEDFs for different mixture compositions and vibrational excitation degrees in CO₂-Ar mixtures, for E/N in the range of 10–100 Td. The high-energy tail of the EEDF is significantly populated as the CO₂ fraction in the mixture decreases, especially at low E/N . This is attributed to the high excitation energy thresholds of inelastic processes in Argon (above 11 eV) and smaller excitation CSs, making it more difficult to transfer electron energy into the excitation channels in Ar than in CO₂. At low E/N , the population of high-energy electrons is relatively low, exacerbating the differences in the shapes of the EEDFs for different mixture compositions. The increase in the vibrational excitation degree enhances the high-energy tails of the EEDF due to the effect of superelastic collisions with vibrationally excited states [54, 55]. In addition, the influence of mixture composition and vibrational temperatures on the shape of the EEDFs is attenuated at high E/N , as the applied field drives the electrons to high energy regions, where the differences between the global CSs of the two gases are less pronounced.

The CO₂ dissociation rate coefficients as a function of E/N are shown in figures 9(a) and (b). The results obtained using the Phelps CSs (case A in table 1) and Polak CSs (case B in

table 1) as CO₂ dissociation CSs are performed by the workflow in figure 5(a) to guarantee the same EEDF as the new workflow (cf figure 5(b)) using the updated CS set in this work. Both the increase of the Ar fraction and the vibrational excitation degree enhance the tail of the EEDF and lead to an increase in the electron-impact dissociation rate coefficient k_{dissoc} . This prediction is consistent with the reported experimental results [67, 75, 79] that show an increase in the CO₂ conversion with the addition of Ar to CO₂ plasmas. It is worth noting that the influence of mixture composition on k_{dissoc} can be neglected once E/N exceeds 500 Td as shown in figure 9(a), due to the saturated transfer of electron energy to the CO₂ dissociation channel at high E/N . The rate coefficient k_{dissoc} calculated with the updated CS set lies between the results of Phelps and Polak CSs and for pure CO₂ is close to the one of Polak CSs at $E/N \lesssim 80$ Td and to the Phelps CSs at $E/N \gtrsim 300$ Td.

We have verified that the proximity of the new results of CO₂ dissociation rate coefficient with the ones obtained with Polak and Slovetsky's CSs [42], for moderate E/N , ensures that self-consistent calculations made with the updated CS set lead to nearly the same results as in our previous works [34, 37, 54–56], within a relative error of 5% in the CO₂ dissociation fraction, difficult to distinguish in a figure. However, for larger Ar fraction the differences between k_{dissoc} obtained with the present updated set and Polak CSs are apparent at lower values of E/N , indicating that in this case the choice of the CO₂ dissociation CSs may play an important role in the calculation of dissociation fractions in CO₂-Ar mixtures. New experiments in CO₂-Ar mixtures may help to further clarify and validate the accuracy of the CO₂ dissociation CSs presented in this work.

4.2. CO₂-N₂ mixtures

The EEDFs at different mixture compositions and vibrational excitation degrees in CO₂-N₂ mixtures are shown in figures 10(a) and (b). In contrast to CO₂-Ar mixtures, a decrease in the CO₂ fraction contributes to the depletion of the population of high-energy electrons and the EEDF tails, due to the low energy threshold for N₂ inelastic processes of ~ 0.3 eV (vibrational excitation) and total excitation CSs larger than that of CO₂. Moreover, the influence of mixture composition on the shape of EEDFs is intensified when the vibrational excitation degree increases, as a consequence of superelastic collisions with vibrationally excited nitrogen [104, 111–113].

Figures 11(a) and (b) show the CO₂ dissociation rate coefficients calculated using the three different CO₂ dissociation CSs for various CO₂-N₂ mixtures compositions. Both the increase of CO₂ fraction and of the vibrational excitation degree in the mixtures can enhance the EEDF and lead to a higher k_{dissoc} . As in the case of CO₂-Ar mixtures, for moderate values of E/N below ~ 80 Td the CO₂ dissociation rate coefficient calculated from the present updated set is close to the one obtained by integration of the EEDF over Polak CSs. However, as the CO₂ fraction decreases the deviation occurs at higher values of E/N , as opposed to the CO₂-Ar mixtures.

Although the addition of N₂ to CO₂ leads to a decrease in k_{dissoc} , the CO₂ absolute conversion increases with the

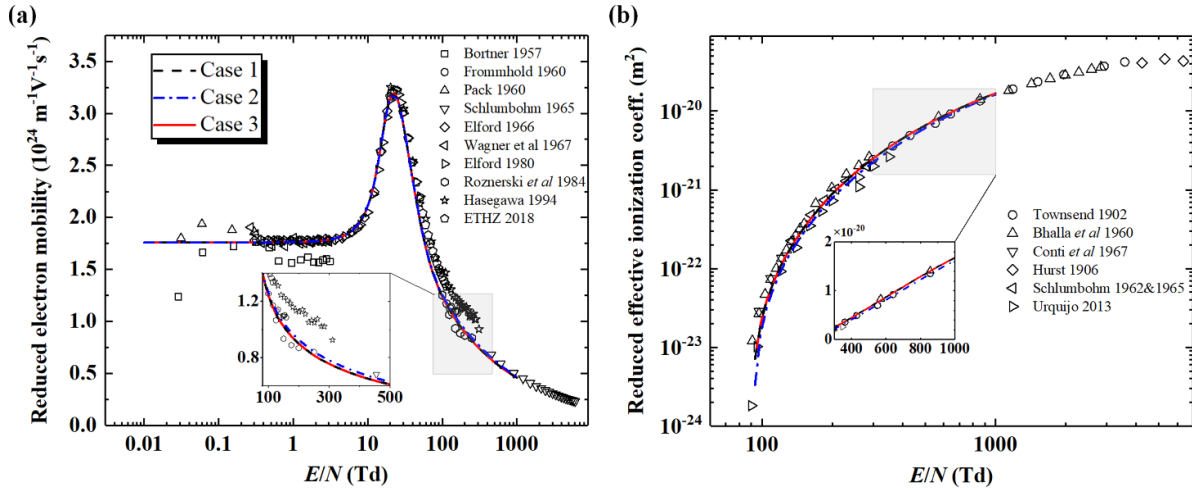


Figure 7. The calculated and measured values [85–101] of electron transport coefficients: (a) reduced electron mobility, (b) reduced effective ionization.

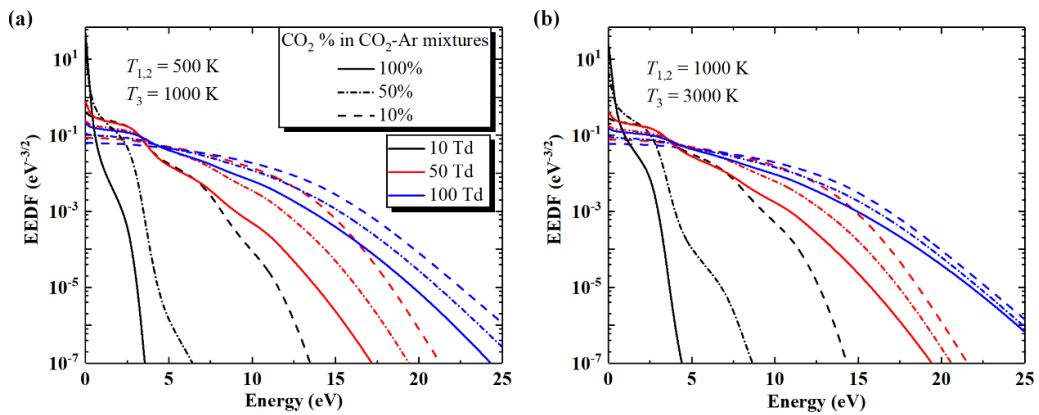


Figure 8. EEDFs at different mixture compositions and vibrational excitation degrees in CO₂–Ar mixtures, for $E/N = 10, 50,$ and 100 Td, for two cases of vibrational temperatures ($T_{1,2}, T_3$): (a) 500 K and 1000 K, (b) 1000 K and 3000 K.

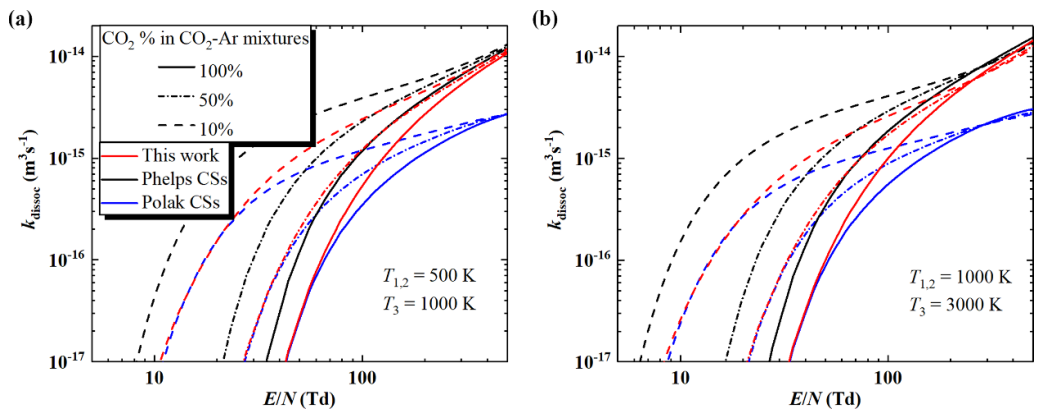


Figure 9. Electron-impact CO₂ dissociation rate coefficients using three sets of CO₂ dissociation CSs at different mixture compositions in CO₂–Ar mixtures, for two cases of vibrational temperatures ($T_{1,2}, T_3$): (a) 500 K and 1000 K, (b) 1000 K and 3000 K.

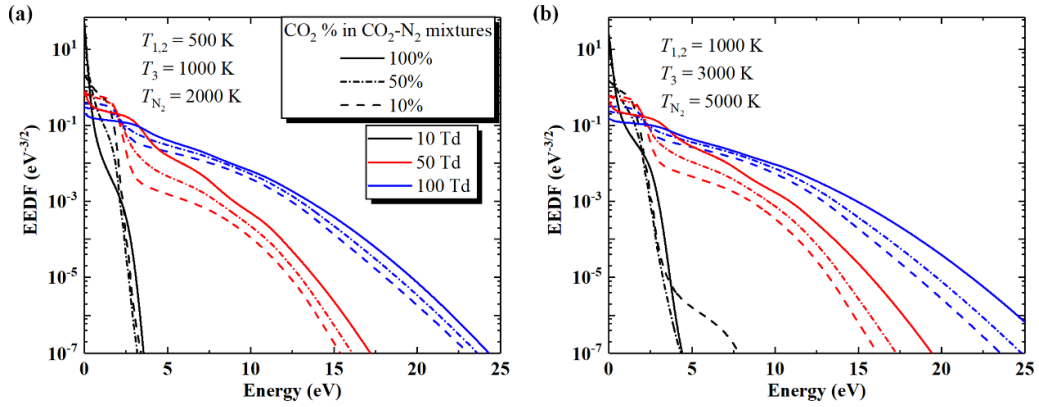


Figure 10. EEDFs at different mixture compositions and vibrational excitation degrees in CO₂-N₂ mixtures, for $E/N = 10, 50,$ and 100 Td, for two cases of vibrational temperatures ($T_{1,2}, T_3, T_{N_2}$): (a) 500 K, 1000 K, and 2000 K, (b) 1000 K, 3000 K, and 5000 K.

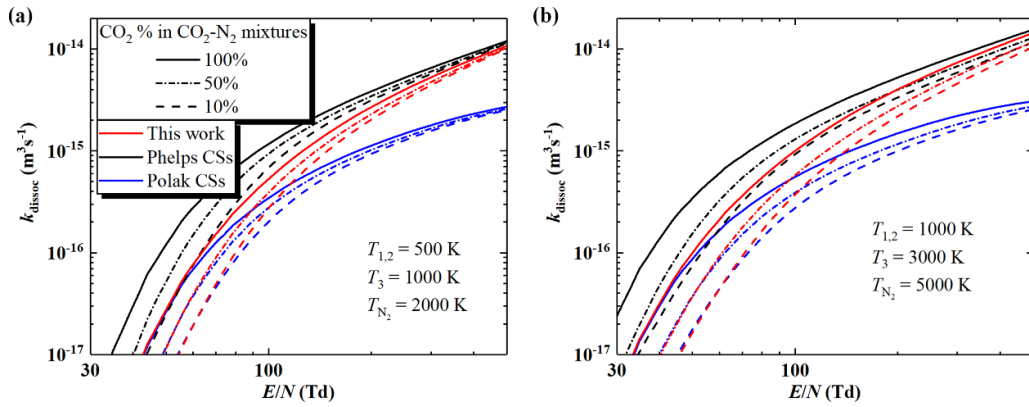


Figure 11. Electron-impact CO₂ dissociation rate coefficients using three sets of CO₂ dissociation CSs at different mixture compositions in CO₂-N₂ mixtures, for two case of vibrational temperatures ($T_{1,2}, T_3, T_{N_2}$): (a) 500 K, 1000 K, and 2000 K, (b) 1000 K, 3000 K, and 5000 K.

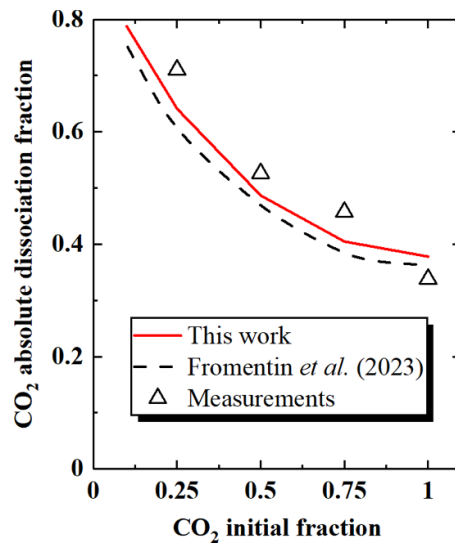


Figure 12. Comparison of the absolute CO₂ absolute dissociation fraction calculated using the present updated set with reported simulation results and measurements [37] in CO₂-N₂ mixtures.

fraction of N_2 in the mixture, owing to the vibrational energy exchanges in CO_2-N_2 and $CO-N_2$ collisions and the limitation of the inverse dissociation reaction [37]. It is worth noting that the calculated CO_2 conversion adopting Polak CSs as CO_2 dissociation channels in a self-consistent model for CO_2-N_2 mixtures under glow discharges conditions slightly underestimates the experimental measurements [37], while the measured E/N is in the range of 75 Td to 125 Td. We have verified the impact of using the updated set in these conditions. Figure 12 illustrates a comparison of the CO_2 absolute dissociation fraction, defined as the ratio of the concentrations of CO to CO_2 and CO in CO_2-N_2 mixtures (i.e. $n_{CO}/(n_{CO} + n_{CO_2})$), when k_{dissoc} is calculated using the updated CS set for CO_2 as compared with Polak's dissociation CSs as in [37]. The differences are not very significant and all the conclusions from Fromentin *et al* [37] remain valid, but it can be noted that the update set leads to a slightly better agreement with experiment.

5. Conclusion

In this work, we update the set of electron-impact CSs for CO_2 from the IST-Lisbon database at LXCat by quantitatively identifying CO_2 dissociation within the electronic excitation channels, and this updated set is validated with measured data over a wide range of E/N . A 15% dissociation branching ratio is set to the electronic excitation CS with threshold at 7 eV proposed by Phelps, associated here with the formation of $O(^1D) + CO(X)$, while the whole Phelps' excitation CS with threshold at 10.5 eV is associated with dissociation into $O(^3P) + CO(a^3\Pi_r)$. Thereby, the updated CS set takes into account explicitly both dissociation and electronic excitation processes, contrary to most consistent sets available in the literature. The separation of the dissociation from the electronic excitation channels enables a full coupling between the electron and chemical kinetics, where the same CSs used to obtain the EEDF are used in the solution of the rate balance equations for the heavy-particles.

Through analysis and assessment of the CO_2 dissociation rate coefficients at moderate E/N ($\lesssim 110$ Td) and the CO_2 conversion efficiencies at high E/N ($\gtrsim 110$ Td), it is confirmed that the updated set of electron-impact CSs gives calculated electron-impact dissociation rate coefficients in excellent agreement with the measured values over a wide range of E/N . Hence, the updated CS set, made available at the IST-Lisbon database within LXCat, prevents the underestimation of the dissociation rate coefficients at high E/N when using Polak's CSs, and its overestimation at low E/N when using Phelps' CSs. Moreover, the reproduction of measured electron transport coefficients when the updated set of electron-impact CSs is used in a Boltzmann solver indicates that the set is consistent.

For moderate reduced electric fields (E/N lower than ~ 80 Td), the calculated dissociation rate coefficients in pure CO_2 are similar to the ones obtained by integrating Polak's dissociation CSs with the EEDF. This similarity ensures the

compatibility of the results of self-consistent models for low-pressure DC discharges in pure CO_2 developed using Polak's dissociation CS with models using the dissociation CSs proposed in this work. A similar compatibility is extended to the case of CO_2-N_2 mixtures, where the new CSs slightly improve the agreement with experiments.

The effects of mixture composition and vibrational excitation degrees on the electron kinetics in CO_2 plasmas with Ar and N_2 admixtures are systematically investigated to extend the application of the updated CO_2 CS set. In CO_2 -Ar mixtures, the high-energy tail of the EEDF is more populated as the CO_2 fraction decreases, and the influence of the mixture composition on the shape of the EEDF is attenuated with increasing vibrational excitation; these trends are opposite in CO_2-N_2 mixtures. In CO_2 -Ar mixtures, as the Ar fraction increases the deviations between the calculated dissociation rate coefficients using Polak's CS or the CSs from this work emerge at lower values of E/N than in pure CO_2 ; in CO_2-N_2 mixtures, as the N_2 fraction increases these deviations manifest at higher values of E/N . This behaviour suggest that new experiments in CO_2 -Ar mixtures can bring additional information on the correctness of the choice of the CO_2 electron-impact dissociation CSs proposed here.

Data availability statement

All data that support the findings of this study are included within the article (and any supplementary files).

Acknowledgment

IPFN activities were funded by FCT (Fundação para a Ciência e a Tecnologia) under projects UIDB/50010/2020, UIDP/50010/2020, LA/P/0061/2020 and PTDC/FIS-PLA/1616/2021 (PARADiSE) (<https://doi.org/10.54499/UIDB/50010/2020>)(<https://doi.org/10.54499/UIDP/50010/2020>)(<https://doi.org/10.54499/LA/P/0061/2020>)(<https://doi.org/10.54499/PTDC/FIS-PLA/1616/2021>). and grant PD/BD/150414/2019 (PD-F APPLAUSE). PV acknowledges support by project CEECIND/00025/2022 of FCT.

In addition, this work was partially funded by the China Scholarship Council (CSC) and Environment and Conservation Fund of Hong Kong Government (Environmental Research, Technology Demonstration and Conference Projects; Project No. 26/2022).

ORCID iDs

Yang Liu  <https://orcid.org/0000-0003-0275-6525>
Tiago Silva  <https://orcid.org/0000-0001-9046-958X>
Tiago C Dias  <https://orcid.org/0000-0002-2179-1345>
Pedro Viegas  <https://orcid.org/0000-0002-3820-3300>
Xiangen Zhao  <https://orcid.org/0000-0002-8476-2103>
Vasco Guerra  <https://orcid.org/0000-0002-6878-6850>

References

- [1] Snoeckx R and Bogaerts A 2017 Plasma technology—a novel solution for CO₂ conversion? *Chem. Soc. Rev.* **46** 5805–63
- [2] Nathanael A J, Kannaiyan K, Kunhiraman A K, Ramakrishna S and Kumaravel V 2021 Global opportunities and challenges on net-zero CO₂ emissions towards a sustainable future *React. Chem. Eng.* **6** 2226–47
- [3] Baldry M, GuriEFF N and Keogh D 2022 Imagining sustainable human ecosystems with power-to-x *in-situ* resource utilisation technology *Acta Astronaut.* **192** 190–8
- [4] George A, Shen B, Craven M, Wang Y, Kang D, Wu C and Tu X 2021 A review of non-thermal plasma technology: a novel solution for CO₂ conversion and utilization *Renew. Sustain. Energy Rev.* **135** 109702
- [5] Guerra V, Silva T, Ogloblina P, Grofulović M, Terraz L, da Silva M L, Pintassilgo C D, Alves L L and Guaitella O 2017 The case for *in situ* resource utilisation for oxygen production on Mars by non-equilibrium plasmas *Plasma Sources Sci. Technol.* **26** 11LT01
- [6] Guerra V, Silva T, Pinhão N, Guaitella O, Guerra-Garcia C, Peeters F J J, Tsampas M N and van de Sanden M C M 2022 Plasmas for *in situ* resource utilization on Mars: fuels, life support, and agriculture *J. Phys. D: Appl. Phys.* **132** 070902
- [7] Alhemeiri N, Kosca L, Gacesa M and Polychronopoulou K 2024 Advancing *in-situ* resource utilization for earth and space applications through plasma CO₂ catalysis *J. CO₂ Util.* **85** 102887
- [8] Kelly S, Verheyen C, Cowley A and Bogaerts A 2022 Producing oxygen and fertilizer with the Martian atmosphere by using microwave plasma *Chem* **8** 2797–816
- [9] Fridman A 2008 *Plasma Chemistry* (Cambridge University Press)
- [10] Bogaerts A and Neyts E C 2018 Plasma technology: an emerging technology for energy storage *ACS Energy Lett.* **3** 1013–27
- [11] Li S, Ongis M, Manzolini G and Gallucci F 2021 Non-thermal plasma-assisted capture and conversion of CO₂ *Chem. Eng. J.* **410** 128335
- [12] Mei D, Zhu X, Wu C, Ashford B, Williams P T and Tu X 2016 Plasma-photocatalytic conversion of CO₂ at low temperatures: understanding the synergistic effect of plasma-catalysis *Appl. Catal. B* **182** 525–32
- [13] Chen G, Britun N, Godfroid T, Georgieva V, Snyders R and Delplancke-Ogletree M P 2017 An overview of CO₂ conversion in a microwave discharge: the role of plasma-catalysis *J. Phys. D: Appl. Phys.* **50** 084001
- [14] Zhang H, Li X, Zhu F, Cen K, Du C and Tu X 2017 Plasma assisted dry reforming of methanol for clean syngas production and high-efficiency CO₂ conversion *Chem. Eng. J.* **310** 114–9
- [15] Bogaerts A et al 2020 The 2020 plasma catalysis roadmap *J. Phys. D: Appl. Phys.* **53** 443001
- [16] Zhang H, Tan Q, Huang Q, Wang K, Tu X, Zhao X, Wu C, Yan J and Li X 2022 Boosting the conversion of CO₂ with biochar to clean CO in an atmospheric plasmatron: a synergy of plasma chemistry and thermochemistry *ACS Sustain. Chem. Eng.* **10** 7712–25
- [17] Ray D, Ye P, Yu J C and Song C 2023 Recent progress in plasma-catalytic conversion of CO₂ to chemicals and fuels *Catal. Today* **423** 113973
- [18] Guerra V and Loureiro J M A H 1997 Electron and heavy particle kinetics in a low-pressure nitrogen glow discharge *Plasma Sources Sci. Technol.* **6** 361
- [19] Kolobov V I and Arslanbekov R R 2006 Simulation of electron kinetics in gas discharges *IEEE Trans. Plasma Sci.* **34** 895–909
- [20] Capitelli M, Celiberto R, Colonna G, Esposito F, Gorse C, Hassouni K, Laricchiuta A and Longo S 2016 *Fundamental Aspects of Plasma Chemical Physics: Kinetics* (Springer)
- [21] Bartschat K and Kushner M J 2016 Electron collisions with atoms, ions, molecules, and surfaces: fundamental science empowering advances in technology *Proc. Natl Acad. Sci.* **113** 7026–34
- [22] Bartschat K 2018 Electron collisions—experiment, theory, and applications *J. Phys. B: At. Mol. Opt. Phys.* **51** 132001
- [23] Hagelaar G J M and Pitchford L C 2005 Solving the Boltzmann equation to obtain electron transport coefficients and rate coefficients for fluid models *Plasma Sources Sci. Technol.* **14** 722
- [24] Stephens J 2018 A multi-term Boltzmann equation benchmark of electron-argon cross-sections for use in low temperature plasma models *J. Phys. D: Appl. Phys.* **51** 125203
- [25] Flynn M, Neuber A and Stephens J 2021 Benchmarking the calculation of electrically insulating properties of complex gas mixtures using a multi-term Boltzmann equation model *J. Appl. Phys.* **55** 015201
- [26] Tejero-del-Caz A, Guerra V, Gonçalves D, da Silva M L, Marques L, Pinhão N, Pintassilgo C D and Alves L L 2019 The lisbon kinetics Boltzmann solver *Plasma Sources Sci. Technol.* **28** 043001
- [27] Tejero-del-Caz A, Guerra V, Pinhão N, Pintassilgo C D and Alves L L 2021 On the quasi-stationary approach to solve the electron Boltzmann equation in pulsed plasmas *Plasma Sources Sci. Technol.* **30** 065008
- [28] Rabie M and Franck C M 2016 METHES: a Monte Carlo collision code for the simulation of electron transport in low temperature plasmas *Comput. Phys. Commun.* **203** 268–77
- [29] Dias T C, Tejero-del-Caz A, Alves L L and Guerra V 2023 The lisbon kinetics Monte Carlo solver *Comput. Phys. Commun.* **282** 108554
- [30] Park R, Scheiner B and Zammit M C 2024 ThunderBoltz: an open-source direct simulation Monte Carlo Boltzmann solver for plasma transport, chemical kinetics, and 0D modeling *Plasma Sources Sci. Technol.* **33** 095007
- [31] Grofulović M, Alves L L and Guerra V 2016 Electron-neutral scattering cross sections for CO₂: a complete and consistent set and an assessment of dissociation *J. Phys. D: Appl. Phys.* **49** 395207
- [32] Alves L L 2014 The IST-LISBON database on LXCat *J. Phys.: Conf. Ser.* **565** 012007
- [33] Pitchford L C et al 2017 Lxcat: an open-access, web-based platform for data needed for modeling low temperature plasmas *Plasma Process. Polym.* **14** 1600098
- [34] Fromentin C, Silva T, Dias T C, Morillo-Candas A S, Biondo O, Guaitella O and Guerra V 2023 Study of vibrational kinetics of CO₂ and CO in CO₂-O₂ plasmas under non-equilibrium conditions *Plasma Sources Sci. Technol.* **32** 024001
- [35] Ogloblina P, Tejero-del-Caz A, Guerra V and Alves L L 2019 Electron impact cross sections for carbon monoxide and their importance in the electron kinetics of CO₂-CO mixtures *Plasma Sources Sci. Technol.* **29** 015002
- [36] Bagheri B, Teunissen J and Ebert U 2020 Simulation of positive streamers in CO₂ and in air: the role of photoionization or other electron sources *Plasma Sources Sci. Technol.* **29** 125021
- [37] Fromentin C, Silva T, Dias T C, Baratte E, Guaitella O and Guerra V 2023 Validation of non-equilibrium kinetics in CO₂-N₂ plasmas *Plasma Sources Sci. Technol.* **32** 054004
- [38] Budde M and Engeln R 2024 Influence of energy transfer processes on the rovibrational characteristics of CO₂ in

- low-temperature conversion plasma with Ar and He admixture *J. Chem. Phys.* **160** 244307
- [39] Pietanza L D, Colonna G and Capitelli M 2024 Self-consistent state-to-state kinetic modeling of CO₂ cold plasmas: insights on the role of electronically excited states *Plasma Chem. Plasma Process.* **44** 1431–68
- [40] Morillo-Candas A S, Klarenaar B L M, Guerra V and Guaitella O 2023 Fast O atom exchange diagnosed by isotopic tracing as a probe of excited states in nonequilibrium CO₂–CO–O₂ Plasmas *J. Phys. Chem. C* **127** 6135–51
- [41] Biagi database 2014 Transcribed from Magboltz version 10.6 (available at: www.lxcat.net/Biagi)
- [42] Polak L S and Slovetsky D I 1976 Electron impact induced electronic excitation and molecular dissociation *Int. J. Radiat. Phys. Chem.* **8** 257–82
- [43] Itikawa Y 2002 Cross sections for electron collisions with carbon dioxide *J. Phys. Chem. Ref. Data* **31** 749–67
- [44] Cosby P C and Helm H 1992 Dissociation rates of diatomic molecules and cells *Report No. MP 92–280* (SRI International)
- [45] Corvin K K and Corrigan S J B 1969 Dissociation of carbon dioxide in the positive column of a glow discharge *J. Chem. Phys.* **50** 2570–4
- [46] Lowke J J, Phelps A V and Irwin B W 1973 Predicted electron transport coefficients and operating characteristics of CO₂–N₂–He laser mixtures *J. Appl. Phys.* **44** 4664–71
- [47] Babaeva N Y and Naidis G V 2021 On the efficiency of CO₂ conversion in corona and dielectric-barrier discharges *Plasma Sources Sci. Technol.* **30** 03LT03
- [48] Bogaerts A, Wang W, Berthelot A and Guerra V 2016 Modeling plasma-based CO₂ conversion: crucial role of the dissociation cross section *Plasma Sources Sci. Technol.* **25** 055016
- [49] Pietanza L D, Colonna G, D'Ammando G, Laricchiuta A and Capitelli M 2015 Vibrational excitation and dissociation mechanisms of CO₂ under non-equilibrium discharge and post-discharge conditions *Plasma Sources Sci. Technol.* **24** 042002
- [50] Pietanza L D, Colonna G, Laporta V, Celiberto R, D'Ammando G, Laricchiuta A and Capitelli M 2016 Influence of electron molecule resonant vibrational collisions over the symmetric mode and direct excitation-dissociation cross sections of CO₂ on the electron energy distribution function and dissociation mechanisms in cold pure CO₂ plasmas *J. Phys. Chem. A* **120** 2614–28
- [51] Pietanza L D et al 2021 Advances in non-equilibrium CO₂ plasma kinetics: a theoretical and experimental review *Eur. Phys. J. D* **75** 237
- [52] Song M Y, Cho H, Karwasz G P, Kokoouline V and Tennyson J 2024 Cross sections for electron collisions with the CO₂ molecule and CO₂⁺ molecular ion *J. Phys. Chem. Ref. Data* **53** 033102
- [53] Morillo-Candas A S, Silva T, Klarenaar B L M, Grofulović M, Guerra V and Guaitella O 2020 Electron impact dissociation of CO₂ *Plasma Sources Sci. Technol.* **29** 01LT01
- [54] Silva A F, Morillo-Candas A S, Tejero-del-Caz A, Alves L L, Guaitella O and Guerra V 2020 A reaction mechanism for vibrationally-cold low-pressure CO₂ plasmas *Plasma Sources Sci. Technol.* **29** 125020
- [55] Ogloblina P, Morillo-Candas A S, Silva A F, Silva T, Tejero-del-Caz A, Alves L L, Guaitella O and Guerra V 2021 Mars *in situ* oxygen and propellant production by non-equilibrium plasmas *Plasma Sources Sci. Technol.* **30** 065005
- [56] Silva T, Morillo-Candas A S, Guaitella O and Guerra V 2021 Modeling the time evolution of the dissociation fraction in low-pressure CO₂ plasmas *J. CO₂ Util.* **53** 101719
- [57] Vialetto L, Viegas P, Longo S and Diomede P 2020 Benchmarking of Monte Carlo flux simulations of electrons in CO₂ *Plasma Sources Sci. Technol.* **29** 115006
- [58] Pokrovskiy G V, Popov N A and Starikovskaia S M 2022 Fast gas heating and kinetics of electronically excited states in a nanosecond capillary discharge in CO₂ *Plasma Sources Sci. Technol.* **31** 035010
- [59] Biondo O, Fromentin C, Silva T, Guerra V, van Rooij G and Bogaerts A 2022 Insights into the limitations to vibrational excitation of CO₂: validation of a kinetic model with pulsed glow discharge experiments *Plasma Sources Sci. Technol.* **31** 074003
- [60] Owen T, Biemann K, Rushneck D R, Biller J E, Howarth D W and Lafleur A L 1977 The composition of the atmosphere at the surface of Mars *J. Geophys. Res.* **82** 4635–9
- [61] Pepin R O 1994 Evolution of the Martian atmosphere *Icar* **111** 289–304
- [62] Boffard J B, Lin C C and De Joseph Jr C A 2004 Application of excitation cross sections to optical plasma diagnostics *J. Phys. D: Appl. Phys.* **37** R143
- [63] Silva T, Britun N, Godfroid T, van der Mullen J and Snyders R 2016 Study of Ar and Ar-CO₂ microwave surfguide discharges by optical spectroscopy *J. Appl. Phys.* **119** 173302
- [64] Songolzadeh M, Soleimani M, Takht Ravanchi M and Songolzadeh R 2014 Carbon dioxide separation from flue gases: a technological review emphasizing reduction in greenhouse gas emissions *Sci. World J.* **2014** 828131
- [65] Bains P, Psarras P and Wilcox J 2017 CO₂ capture from the industry sector *Prog. Energy Combust. Sci.* **63** 146–72
- [66] Heijckers S, Snoeckx R, Kozak T S, Silva T, Godfroid T, Britun N, Snyders R and Bogaerts A 2015 Snyders R and Bogaerts A 2015 CO₂ conversion in a microwave plasma reactor in the presence of N₂: elucidating the role of vibrational levels *J. Phys. Chem. C* **119** 12815–28
- [67] Ramakers M, Michielsen I, Aerts R, Meynen V and Bogaerts A 2015 Effect of argon or helium on the CO₂ conversion in a dielectric barrier discharge *Plasma Process. Polym.* **12** 755–63
- [68] Snoeckx R, Heijckers S, Van Wesenbeeck K, Lenaerts S and Bogaerts A 2016 CO₂ conversion in a dielectric barrier discharge plasma: N₂ in the mix as a helping hand or problematic impurity? *Energy Environ. Sci.* **9** 999–1011
- [69] Ray D, Saha R and Ch S 2017 DBD plasma assisted CO₂ decomposition: influence of diluent gases *Catalysts* **7** 244
- [70] Grofulović M, Klarenaar B L M, Guaitella O, Guerra V and Engeln R 2019 A rotational Raman study under non-thermal conditions in pulsed CO₂–N₂ and CO₂–O₂ glow discharges *Plasma Sources Sci. Technol.* **28** 045014
- [71] Terraz L, Silva T, Morillo-Candas A, Guaitella O, Tejero-del-Caz A, Alves L L and Guerra V 2019 Influence of N₂ on the CO₂ vibrational distribution function and dissociation yield in non-equilibrium plasmas *J. Phys. D: Appl. Phys.* **53** 094002
- [72] Barkhordari A, Mirzaei S I, Falahat A and Rodero A 2021 Numerical and experimental study of an Ar/CO₂ plasma in a point-to-plane reactor at atmospheric pressure *Spectrochim. Acta B* **177** 106048
- [73] Martinez H, Perusquia S, Villa M, Reyes P G, Yousif F B, Castillo F and Contreras U 2017 Study of DC Ar–CO₂ mixture plasma using optical emission spectroscopy and mass spectrometry techniques *Phys. Plasmas* **24** 043508
- [74] Naidis G V and Babaeva N Y 2022 Modeling of CO₂ conversion in low-pressure glow discharges in CO₂–N₂ mixtures *J. Appl. Phys.* **55** 335202

- [75] Xu S, Whitehead J C and Martin P A 2017 CO₂ conversion in a non-thermal, barium titanate packed bed plasma reactor: the effect of dilution by Ar and N₂ *Chem. Eng. J.* **327** 764–73
- [76] Capitelli M, Colonna G, D'Ammando G and Pietanza L D 2017 Self-consistent time dependent vibrational and free electron kinetics for CO₂ dissociation and ionization in cold plasmas *Plasma Sources Sci. Technol.* **26** 055009
- [77] Beuthe T G and Chang J S 1997 Chemical kinetic modelling of non-equilibrium Ar-CO₂ thermal plasmas *Jpn. J. Appl. Phys.* **36** 4997
- [78] Horvath G, Skalný J D and Mason N J 2008 FTIR study of decomposition of carbon dioxide in dc corona discharges *J. Phys. D: Appl. Phys.* **41** 225207
- [79] Moss M S, Yanallah K, Allen R W K and Pontiga F 2017 An investigation of CO₂ splitting using nanosecond pulsed corona discharge: effect of argon addition on CO₂ conversion and energy efficiency *Plasma Sources Sci. Technol.* **26** 035009
- [80] Ozkan A, Dufour T, Silva T, Britun N, Snyders R, Reniers F and Bogaerts A 2016 DBD in burst mode: solution for more efficient CO₂ conversion? *Plasma Sources Sci. Technol.* **25** 055005
- [81] Legasov V A, Vakar A K, Denisenko V P, Maksimov G P, Rusanov V D, Fridman A A and Sholin G V 1978 Plasma radiolysis of carbon dioxide gas by heavy current beam of relativistic electrons *Dokl. Akad. Nauk* **243** 323–5
- [82] van den Bekerom D C, Linares J P, Verreycken T, Van Veldhuizen E M, Nijdam S, Berden G, Bongers W A, Van De Sanden M C and van Rooij G J 2019 The importance of thermal dissociation in CO₂ microwave discharges investigated by power pulsing and rotational Raman scattering *Plasma Sources Sci. Technol.* **28** 055015
- [83] Montesano C, Salden T P, Martini L M, Dilecce G and Tosi P 2023 CO₂ reduction by nanosecond-plasma discharges: revealing the dissociation's time scale and the importance of pulse sequence *J. Phys. Chem. C* **127** 10045–50
- [84] Laporta V, Tennyson J and Celiberto R 2016 Calculated low-energy electron-impact vibrational excitation cross sections for CO₂ molecule *Plasma Sources Sci. Technol.* **25** 06LT02
- [85] Bortner T E, Hurst G S and Stone W G 1957 Drift velocities of electrons in some commonly used counting gases *Rev. Sci. Instrum.* **28** 103–8
- [86] Frommhold L 1960 Eine untersuchung der elektronenkomponente von elektronenlawinen im homogenen feld II *Z. Phys.* **160** 554–67
- [87] Pack J L, Voshall R E and Phelps A V 1962 Drift velocities of slow electrons in krypton, xenon, deuterium, carbon monoxide, carbon dioxide, water vapor, nitrous oxide, and ammonia *Phys. Rev.* **127** 2084
- [88] Schlumbohm H 1962 Elektronenlawinen in elektronegativen gasen: zur gleichzeitigen messung des stoßionisierungs- und anlagerungskoeffizienten α und η für elektronen und der geschwindigkeiten positiver und negativer Ionen *Z. Phys.* **166** 192–206
- [89] Schlumbohm H 1965 Messung der driftgeschwindigkeiten von elektronen und positiven Ionen in gasen *Z. Phys.* **182** 317–27
- [90] Schlumbohm H 1965 Stoßionisierungskoeffizient α , mittlere elektronenenergien und die beweglichkeit von elektronen in gasen *Z. Phys.* **184** 492–505
- [91] Elford M T 1966 The drift velocity of electrons in carbon dioxide at 293 K *Aust. J. Phys.* **19** 629
- [92] Wagner E B, Davis F J and Hurst G S 1967 Time-of-Flight investigations of electron transport in some atomic and molecular gases *J. Chem. Phys.* **47** 3138–47
- [93] Elford M T and Haddad G N 1980 The drift velocity of electrons in carbon dioxide at temperatures between 193 and 573 K *Aust. J. Phys.* **33** 517–30
- [94] Roznerski W and Leja K 1984 Electron drift velocity in hydrogen, nitrogen, oxygen, carbon monoxide, carbon dioxide and air at moderate E/N *J. Phys. D: Appl. Phys.* **17** 279
- [95] Nakamura Y 1995 Drift velocity and longitudinal diffusion coefficient of electrons in CO₂? Ar mixtures and electron collision cross sections for CO₂ molecules *Aust. J. Phys.* **48** 357–64
- [96] Haefliger P and Franck C M 2018 Detailed precision and accuracy analysis of swarm parameters from a pulsed Townsend experiment *Rev. Sci. Instrum.* **89** 023114
- [97] Townsend J S 1902 The conductivity produced in gases by the aid of ultra-violet light *London, Edinburgh Dublin Phil. Mag. J. Sci.* **3** 557–76
- [98] Hurst H 1906 Die Entstehung der Ionen durch Zusammenstoß und die Funkenspannung in Kohlendioxyd und Stickstoff *Phil. Mag.* **11** 535
- [99] Bhalla M S and Craggs J D 1960 Measurement of ionization and attachment coefficients in carbon dioxide in uniform fields *Proc. Phys. Soc.* **76** 369
- [100] Conti V J and Williams A W 1967 *Contributed Papers of the Eight Int. Conf. on Phenomena in Ionized Gases (Vienna, 27 August–2 September 1967)* (Springer)
- [101] UNAM database 2015 Electron swarm data derived from a pulsed Townsend experiment at UNAM (available at: www.lxcat.net/UNAM)
- [102] Yanguas-Gil A, Cotrino J and Alves L L 2005 An update of argon inelastic cross sections for plasma discharges *J. Phys. D: Appl. Phys.* **38** 1588
- [103] Coche P, Guerra V and Alves L L 2016 Microwave air plasmas in capillaries at low pressure I. Self-consistent modeling *J. Phys. D: Appl. Phys.* **49** 235207
- [104] Loureiro J and Ferreira C M 1986 Coupled electron energy and vibrational distribution functions in stationary N₂ discharges *J. Phys. D: Appl. Phys.* **19** 17
- [105] Grofulović M, Silva T, Klarenaar B L M, Morillo-Candas A S, Guaitella O, Engeln R, Pintassilgo C D and Guerra V 2018 Kinetic study of CO₂ plasmas under non-equilibrium conditions. II. Input of vibrational energy *Plasma Sources Sci. Technol.* **27** 115009
- [106] Silva T, Grofulović M, Klarenaar B L M, Morillo-Candas A S, Guaitella O, Engeln R, Pintassilgo C D and Guerra V 2018 Kinetic study of low-temperature CO₂ plasmas under non-equilibrium conditions. I. Relaxation of vibrational energy *Plasma Sources Sci. Technol.* **27** 015019
- [107] Adamovich I, Saupé S, Grassi M J, Schulz O, Macheret S and Rich J W 1993 Vibrationally stimulated ionization of carbon monoxide in optical pumping experiments *Chem. Phys.* **173** 491–504
- [108] Babou Y, Rivière P, Perrin M Y and Soufiani A 2008 Spectroscopic study of microwave plasmas of CO₂ and CO₂-N₂ mixtures at atmospheric pressure *Plasma Sources Sci. Technol.* **17** 045010
- [109] Silva T, Britun N, Godfroid T and Snyders R 2014 Optical characterization of a microwave pulsed discharge used for

- dissociation of CO₂ *Plasma Sources Sci. Technol.* **23** 025009
- [110] Damen M A, Martini L M and Engeln R 2020 Temperature evolution in a pulsed CO₂-N₂ glow discharge measured using quantum cascade laser absorption spectroscopy *Plasma Sources Sci. Technol.* **29** 065016
- [111] Capitelli M, Dilonardo M and Gorse C 1981 Coupled solutions of the collisional Boltzmann equations for electrons and the heavy particle master equation in nitrogen *Chem. Phys.* **56** 29–42
- [112] Gorse C, Cacciatore M, Capitelli M, De Benedictis S and Dilecce G 1988 Electron energy distribution functions under N₂ discharge and post-discharge conditions: a self-consistent approach *Chem. Phys.* **119** 63–70
- [113] Capitelli M, Colonna G, D'Ammando G, Laporta V and Laricchiuta A 2013 The role of electron scattering with vibrationally excited nitrogen molecules on non-equilibrium plasma kinetics *Phys. Plasmas* **20** 101609